INNOVARE JOURNAL OF SCIENCES

Vol 6, Issue 2, 2018

ISSN - 2321-5496

Research Article

QUANTUM MECHANICAL DESCRIPTORS OF NILOTINIB'S IMPURITIES

DEBANJAN MITRA*

Department of Biotechnology, The University of Burdwan, Burdwan, West Bengal - 713 104, India. Email: debanjanmitra267@gmail.com

Received: 13 September 2018, Revised and Accepted: 24 September 2018

ABSTRACT

Objective: Mutagenic/genotoxic impurities in the clinically approved drugs have been a major concern for the pharmaceutical industry. Nilotinib (N), which is an approved drug of chronic leukemia, has a number of impurities (nilotinib impurity [NI]-3, NI-5, and NI-12). For drugs, either semi-empirical or quantum mechanical (QM) or topological molecular descriptors (MDs) have been popular for QSAR studies. However, details of MDs for impurities are yet to be established. Thus, the objective of the study has been to compute QM-based MDs for impurities of N and to compare them with that of approved drugs to identify MDs of the former in relation to their known genotoxic/mutagenic properties.

Methods: Impurities are optimized by B3LYP/6-311G (d,p) level of theory and ionization potential (*IP*), electron affinity (*EA*), and other MDs are determined. Further, non-linear optical (NLO) descriptors such as dipole moment (*DM*) and polarizability (α) are also determined.

Results: Impurities of N show much deviation of *IP*, *EA*, *MD*, α, and other properties from the reported mean values of approved drugs. Unlike NI-5 and NI-12, NI-3 shows increase in *DM* (~double) and α properties, which may point to its higher interactivity with cellular targets (like DNA/RNA/protein), might be due to additional substituents, π-conjugation, and planarity in its structure. The latter seems to be due to compensation of oppositely sensed dihedral properties of the structure of NI-3.

Conclusion: The study identifies QM-based differential MDs for impurities of N, which seems to have a relationship with their genotoxicity/mutagenicity properties. Similar studies can be done for other such systems.

Keywords: Genotoxicity, Mutagenicity, Nilotinib, Impurities, Molecular descriptors, Density functional theory, Electronic properties, Non-linear optical properties.

INTRODUCTION

Nilotinib (N) is the next generation drug against specific tyrosine kinase protein, known as Bcr-Abl. White blood cells that harbor Philadelphia chromosome, which is resulted from reciprocal translocation of long arms of chromosomes 9 and 22 [1], are affected with chronic myeloid leukemia (CML). Inhibition of Bcr-Abl kinase protein has been shown to be highly effective in stopping the uncontrolled growth of leukemia cells. N is more effective and selective than imatinib [2], which is used for gastrointestinal and other kinds of malignancies. Chemically, N has both aminopyrimidine and amide parts as imatinib with an additional substituent, for example, trifluoromethyl methylimidazole-phenyl, alternative to the highly basic N-methylpiperazine of imatinib, thereby leading to greater lipophilicity. This structural feature of N not only allows tighter binding to the target but also decreases the effective dose. Notably, N is also used to treat certain other types of CML, where other drug therapies were demonstrated to be non-functional.

Genotoxic impurities may potentially damage cell's genetic materials such as DNA and RNA and thus have been the major concern for pharmaceutical industries [3]. These mutagens may undergo irreversible binding to the nucleic acids/proteins, thereby affect normal cellular processes, induce mutation and cancer, and damage cellular signaling and immune response. These impurities are present in active drug substance and drug products. The International Council for Harmonisation (ICH) and other International Agencies provide guidelines for toxicological assessment for these impurities [4,5]. However, the guidelines apparently have been insufficient with respect to the questions as to which impurities are genotoxic and how their levels are controlled [4,5]. Physicochemical, semi-empirical toxicological assessment is performed through QSAR methodology as per ICH, M7 guidelines [6]. Almost all approved drugs including N for human subjects have been shown to contain numbers of impurities that are associated during their synthesis and subsequent processing and degradation [7].

Chemical reactivity and stability of drug largely depend on their electronic structures. Matuszek and Reynisson (2016) have computed mean values of electronic and non-linear optical (NLO) properties based on a large database of clinically approved drugs using highly accurate quantum mechanical (QM) procedure. Such type of QM descriptors remains to be investigated for genotoxic/mutagenic impurities. N has a number of reported impurities (Table 1) that come as minor peaks in the high-performance liquid chromatography (HPLC) profile [8] similar as in other contexts (such as dasatinib) that are detected and quantified by ultra HPLC technology [9]. Here, we present a detailed characterization of few of the impurities of N using cost-effective density functional computation. The study involves RB3LYP method with 6-311G (d,p) basis set to extract E_{HOMO}, E_{LUMO}, band-gap (ΔE), dipole moment (*DM*), electron affinity (*EA*), ionization potential (*IP*), chemical hardness (η) and softness (σ), chemical potential (μ), and electrophilicity index (ω). Further and importantly, NLO properties such as polarizability (α), the anisotropy of polarizability ($\Delta\alpha$), and first and second rank hyperpolarizability (β and γ respectively) [10] are also been analyzed. These properties are then used to compare between impurities and drugs to gain insight into the origin of toxicity of the former.

METHODS

GAUSSIAN 09 Revision-B.01-SMP [10] and GAUSS VIEW 5.0.9 [11,12] are used as earlier [13] for all computations. Structures were drawn in GAUSS VIEW 5.0.9 [11] of GAUSSIAN [12] software package. Initial structures were cleaned repeatedly to obtain normalized geometry. Each of the N's impurity was then subjected for successive optimization using semi-empirical (PM3), Hartree–Fock, and DFT methods in conjunction with appropriate basis sets. Final optimization of these molecules is achieved using DFT/B3LYP/6-311G (d,p) method. For computation of linear and NLO properties, the additional key of "optical" was included in the study. Following equations are used for the extraction of parameters and properties of these impurities.

Table 1: Structural characteristics of reported mutagenic/genotoxic impurities of nilotinib

Impurity with IUPAC name	Structure
Nilotinib genotoxic impurity 3 (NI-3) [3-amino-4-methyl-N-[3-(4-methylimidazol-1-yl)-5-(trifluoromethyl) phenyl] benzamide]	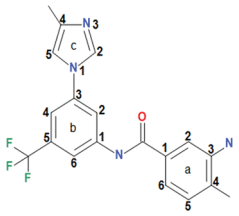
Nilotinib impurity 5 (NI-5) [3-(5-methylimidazol-1-yl)-5-(trifluoromethyl) aniline]	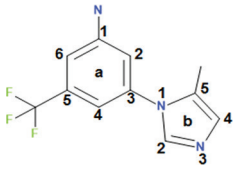
Nilotinib impurity 12 (NI-12) [3-(4-methylimidazol-1-yl)-5-(trifluoromethyl) benzonitrile]	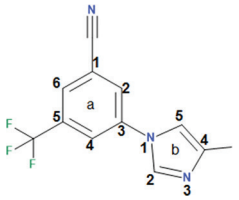

E_{HOMO} and E_{LUMO} are directly extracted from the LOG file of the corresponding optimized structure. The following formula is then used to obtain other dependent QM parameters. *IP* is the amount of energy required to take away one electron from a neutral molecule (*M*) and *EA*, oppositely, is the amount of energy released when an electron is added to an *M*, i.e.,

$$M + I \rightarrow M^{+} + e$$
$$Thus, I = E(M^{+}) - E(M)$$
$$M + e \rightarrow M^{-} + A$$
$$Thus, A = E(M) - E(M^{-}) \quad (1)$$

μ is the ability of a molecule to participate in the chemical reaction. It can either be positive or negative. It is one of the very important parameters for the determination of the reactivity nature of a molecule. It is referred to as negative of electronegativity (χ) which is estimated as:

$$\mu = -\left(\frac{\delta E}{\delta N}\right)_{v} = -\left(\frac{\delta E}{\delta \rho}\right)_{v} = -\left(\frac{I+A}{2}\right);\ \chi = \left(\frac{I+A}{2}\right) \quad (2)$$

η is a very important parameter that allows understanding of the chemical reactivity of a molecule. It is the slope of the curve of μ, in electronic energy (E) versus electron number plot. In other words, η is the curvature of the μ curve. The value is always positive. However, lower the value, the higher the reactivity of the molecule. η and it's reciprocal (i.e., σ) are computed as:

$$\eta = \frac{1}{2}\left(\frac{\delta c}{\delta N}\right)_{v} = \frac{1}{2}\left(\frac{\delta^{2} E}{\delta N^{2}}\right) = \frac{(I-A)}{2};\ \sigma = \frac{1}{\eta} \quad (3)$$

Global electrophilicity index (ω) has been worked out [8] using the μ and η parameters.

$$\omega = \frac{\mu^{2}}{2\eta} \quad (4)$$

While *DM* is the measure of α of a molecule in its ground state, α is the intrinsic capacity of a molecule of having a dipole when it is assaulted with an external electric field.

If an *M* is present in a weak, static electric field (of strength, *F*), then the total energy (E) of the molecule can be express as a Taylors series.

$$E_{F} = E_{0} - \mu_{\alpha} F_{\alpha} - \frac{1}{2!}\alpha_{\alpha\beta} F_{\alpha} F_{\beta} - \frac{1}{3!}\beta_{\alpha\beta\gamma} F_{\alpha} F_{\beta} F_{\gamma} - \frac{1}{4!}\gamma_{\alpha\beta\gamma\delta} F_{\alpha} F_{\beta} F_{\gamma} F_{\delta} - .... \quad (5)$$

E_{0} denotes the energy of the molecule in the absence of an external electrical field. Energy (E_{0}), dipole moment (μ_{α}), polarizability ($\alpha_{\alpha\beta}$), and first- and second-order hyperpolarizability ($\beta_{\alpha\beta\gamma}$ and $\gamma_{\alpha\beta\gamma\delta}$, respectively) denote the molecular properties. Polarizability and first- and second-rank hyperpolarizabilities are expressed as tensor quantities, whereas subscripts single, double, etc., denote the first-rank and second-rank tensor, etc., in Cartesian coordinate.

Now, if the external field lies on any one of the three orthogonal Cartesian axes, then the components of the induced moments will be parallel to the field. In that case, off-diagonal terms of the tensor, $\alpha_{\alpha\beta}$ vanish. Under this conditions, the expected value of α and DMs is obtained as:

$$DM = \sqrt{\left(\mu_{X}^{2} + \mu_{Y}^{2} + \mu_{Z}^{2}\right)} \quad (6)$$

$$\left\langle \alpha_{STATIC} \right\rangle = \frac{\left(\alpha_{XX} + \alpha_{YY} + \alpha_{ZZ}\right)}{3}\ OR\ \left\langle \alpha_{STATIC} \right\rangle = \frac{1}{3} Trace[\alpha] \quad (7)$$

In case of the anisotropic orientation of the external field, the anisotropy of the polarizability (<*Δα*>) can be computed as:

$$\left\langle \Delta\alpha \right\rangle = \left[\frac{\left(\alpha_{XX} - \alpha_{YY}\right)^{2} + \left(\alpha_{YY} - \alpha_{ZZ}\right)^{2} + \left(\alpha_{YY} - \alpha_{ZZ}\right)^{2} + 6\left(\alpha_{XY}^{2} + \alpha_{XY}^{2} + \alpha_{YZ}^{2}\right)}{2}\right]^{\frac{1}{2}} \quad (8)$$

Similarly, the first-order ($\beta_{\alpha\beta\gamma}$) and second-order ($\gamma_{\alpha\beta\gamma\delta}$) hyperpolarizability is calculated from components of respective tensors that are obtained from the GAUSSIAN output file.

$$\left\langle \beta_{STATIC} \right\rangle = \left[\beta_{X}^{2} + \beta_{Y}^{2} + \beta_{Z}^{2}\right]^{\frac{1}{2}}$$

$$\beta_i = \beta_{iii} + \frac{1}{3}\sum_{i \neq k}\left(\beta_{ikk} + \beta_{kik} + \beta_{kki}\right) \quad (9)$$

$$\left\langle \beta_{STATIC} \right\rangle = \begin{bmatrix} \left(\beta_{XXX} + \beta_{XYY} + \beta_{XZZ}\right)^2 \\ +\left(\beta_{YYY} + \beta_{YZZ} + \beta_{YXX}\right)^2 \\ +\left(\beta_{ZZZ} + \beta_{ZXX} + \beta_{ZYY}\right)^2 \end{bmatrix}^{\frac{1}{2}}$$

$$\left\langle \gamma_{STATIC} \right\rangle = \frac{\gamma_{XXXX} + \gamma_{YYYY} + \gamma_{ZZZZ} + 2\gamma_{YYXX} + 2\gamma_{YYZZ} + 2\gamma_{ZZXX}}{5} \quad (10)$$

All these optical terms were calculated using appropriate basis set that contains polarized and diffused functions for high accuracy, in that DFT/B3LYP/6311G(d,p) was preferred.

RESULTS

Although experimental details on the structure of N are available either in pure or the complex form [14,15], little is known about the molecular structure, stability, and chemical reactivity for its impurities. In this study, we have considered three impurities such as nilotinib impurities (NI)-3, NI-5, and NI-12.

Table 2: Pharmacokinetic and ADME properties of nilotinib's impurities along with nilotinib (N)

Name	LogP	PSA (A^2)	nA	HBA	HBD	nrotb	Volume (A^3)
NI-3	3.4	72.9	27	5	3	4	315.1
NI-5	1.8	43.8	17	3	2	2	195.8
NI-12	2.4	41.6	18	3	0	2	201.3
N	4.99	97.6	39	8	2	7	446.6

LogP: Octanol-water partition coefficient (≤5), PSA: Sum of surface of polar atoms (≤140), natoms (≥20 and≤70): Number of atoms, HBA: Hydrogen bond acceptor (≤10), HBD: Hydrogen bond donor (≤5), nrotb: Number of rotatable bonds, vol: Volume, MW: Molecular weight (≤500), ADME: Absorption, distribution, metabolism, and excretion, NI: Nilotinib impurity

Table 3: Bond lengths (in Å) of N and its impurities. The experimental values of the former are extracted from the crystal structure, 3CS9.pdb [15]

Bond length in Å	Nilotinib in 3CS9. pdb	NI-3	NI-5	NI-12
N1-C1	1.338	1.375	1.380	1.379
N1-C2	1.394	1.390	1.395	1.393
N1-C3	1.403	1.417	1.423	1.411
C3-C4	1.391	1.396	1.393	1.398
C3-C5	1.398	1.391	1.395	1.395
N2-C6	1.389	1.402	NA	NA
N2-C7	1.342	1.385	NA	NA
C8-C9	1.371	1.394	NA	NA
C8-C10	1.403	1.399	NA	NA

All measurements are performed using GAUSS VIEW v5.09 [11]. Unavailable bonds are reported as NA, i.e., not available. NI: Nilotinib impurity

Table 4: Angles (in Å) of N and its impurities

Angle in degree	N in 3CS9.pdb	NI-3	IMI5	NI-12
C1-N1-C2	104.155	105.841	106.478	105.792
C1-N1-C3	126.774	126.854	125.237	126.904
C2-N1-C3	128.928	127.289	128.278	127.281
C4-C3-C5	119.501	120.142	120.777	119.685
C6-N2-C7	125.972	128.659	NA	NA
C9-C8-C10	116.299	119.457	NA	NA

All measurements are performed using GAUSS VIEW v5.09 [11]. Unavailable bonds are reported as NA, i.e., not available. The experimental values of the latter are taken from the crystal structure, 3CS9.pdb [15]. N: Nilotinib, NI: Nilotinib impurity

Pharmacokinetics properties

Pharmacokinetic properties for these impurities and N are determined using authentic web service [16], the result of which is presented in Table 2. Following points are noteworthy from the table. First, these pharmacokinetic properties of impurities do not vary much from the original drug (N). Second, none of these impurities violates the upper limit of Lipinski's rule [17,18]. Third, in NI-12, hydrogen bond donor groups are absent, and finally, the numbers of heavy atoms are below the rule in NI-5 and NI-12.

Bond length, angle, and dihedral properties

Quantum mechanically optimized structures are shown in Fig. 1 (upper panel). These are used to determine selective bond lengths (in Å), angles (in degree), and dihedral angles (in degree), the result of which are presented in Tables 3-5, respectively, along with available experimental results for comparison purposes. Common atoms in the structures of these impurities are identified using an arbitrary numbering scheme (Fig. 1). NI-3 has three (A, B, and C) compared to two rings (A and B) in NI-5 and NI-12 (Fig. 1). Following points are noteworthy from these tables.

First, common bond lengths are almost identical (Table 3) for these impurities (NI-3, NI-5, and NI-12), which show variations (underlined; Table 3) when compared with that of N itself (Table 3). Notable, due to lack of the third ring (i.e., ring C) in NI-5 and NI-12, last four bond lengths are not available for comparison purpose. Second, similar to bond lengths, relevant angles are also compared in Table 4. It is seen that N shows slight variations in few of its representative angles when compared with that of the impurities. However, these impurities show remarkable similarities in angles when compared among themselves.

The results of the dihedral angles are presented in Table 5. Several points are noteworthy from the table. First, there are two sets of dihedral angles. Set-1 is comparable among all impurities as well as with N. Set-2 only exists in NI-3 and N. Second, the sense of rotation of the set-1 torsion angle for N, NI-5, and NI-12 is identical, which is counterclockwise. Notably, it is not the case for NI-3, which shows the opposite and clockwise sense. Third, the amount of rotation for this set also varies in that N has the lowest and NI-5 has the highest, which is followed by NI-3 and NI-12. Forth, compare to NI-5 and NI-12, in case of NI-3, additional set (set-2) of dihedral angle exists (Table 5). In set-2, compare to the N, NI-3 largely harbors oppositely sensed dihedral angles.

Optimized structure, electronic parameters, and properties

The highest occupied molecular orbital (HOMO) and lowest occupied molecular orbital (LUMO) for NI-3, NI-5, and NI-12 are presented in Fig. 1, along with their optimized structures. While HOMO delocalizes over bonds of NI-3, NI-5, and NI-12, it is less prominent for C ring of NI-3 and B-ring of NI-12. Notably, the delocalization is uniform in NI-5 (Fig. 1). In turn, the LUMO is mostly located in B- and C-rings for NI-3, A- and B-ring of NI-5, and B-ring of NI-12. By the use of DFT/B3LYP/6-311G (d,p) level of theory, the extracted energies for HOMO, LUMO, and ΔE for NI-3, NI-5, and NI-12 are presented in Table 6 and compared in Fig. 2.

It is clear from the table and figures that electron donating ability (E_{HOMO}) follows the order as NI-5<NI-12<NI-3 (Fig. 2a). Electron-accepting ability (E_{LUMO}) is seen to follow the order as NI-12<NI-3<NI-5 (Fig. 2b). What about the band gap for these molecules? It (Fig. 2c) follows the reverse order of LOMO (Fig. 2b). The chemical reactivity is highest and the kinetic stability is lowest for NI-12, which is followed by NI-3 and NI-5 (Fig. 2c).

We have computed adiabatic *IP* and adiabatic *EA* for NI-3, NI-5, and NI-12 and presented in Table 7 and Fig. 3a and b. It is noteworthy from

Table 5: Comparison of dihedral angle (in degree) of impurities along with N. The experimental values of the latter are taken from the crystal structure, 3CS9.pdb [15]

Dihedral angle in degree	Planes	N in 3CS9.pdb	NI-3	NI-5	NI-12
Set-1					
C1-N1-C3-C4	Between rings - A and B	−18.3	38.7	−53.1	−35.7
C2-N1-C3-C4		156.7	−143.0	125.8	146.3
C1-N1-C3-C5		163.4	−141.1	125.5	144.1
C2-N1-C3-C5		−21.7	37.3	−55.5	−33.9
Set-2					
C5-C6-N2-C7	Between rings B and C through N2 and C7	−154.8	−176.5	NA	NA
N2-C7-C8-C9		165.8	−157.0	NA	NA
N2-C7-C8-C10		−0.4	24.9	NA	NA

All measurements are performed using GAUSS VIEW v5.09 [11]. N: Nilotinib, NI: Nilotinib impurity

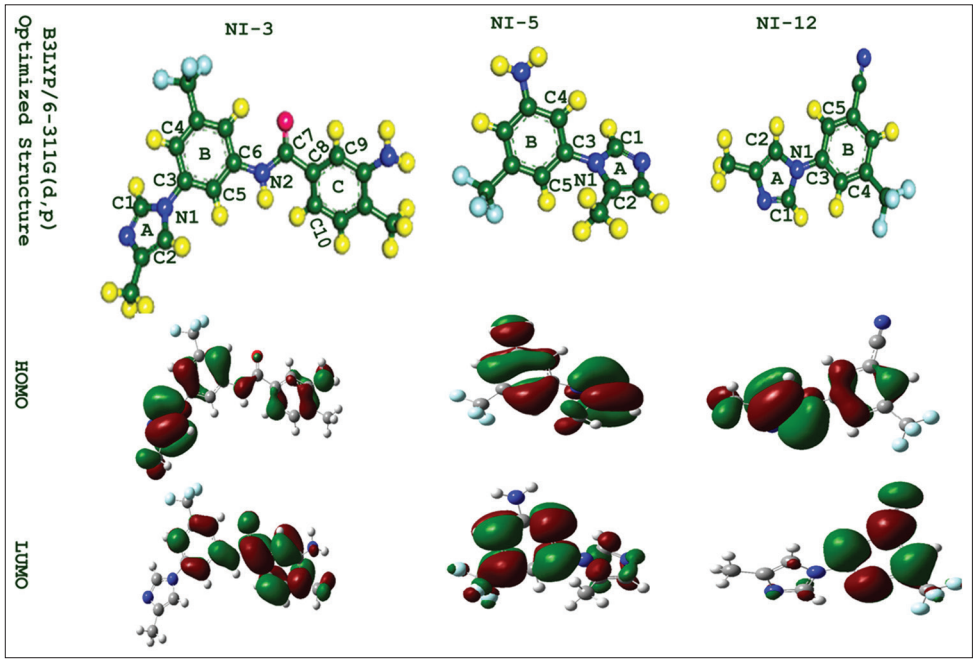

Fig. 1: Energy optimized structures (upper panel) along with highest occupied molecular orbitals (middle panel) and lowest unoccupied molecular orbitals (lower panel) or frontier molecular orbitals of NI-3, NI-5, and NI-12

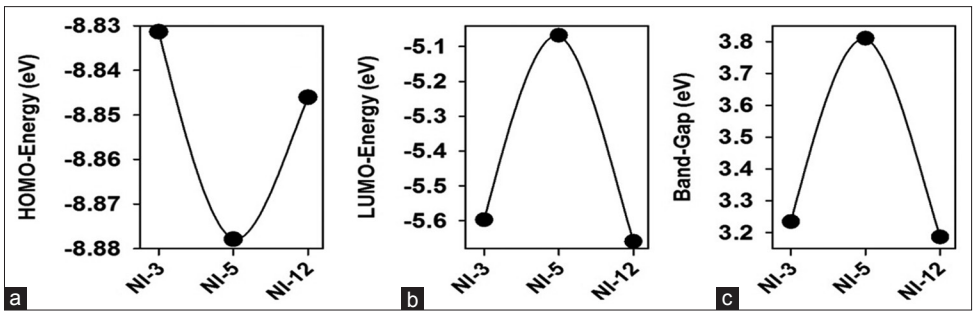

Fig. 2: Plot of highest occupied molecular orbitals (a), lowest unoccupied molecular orbitals (b), and band gap (c) energies for NI-3, NI-5, and NI-12

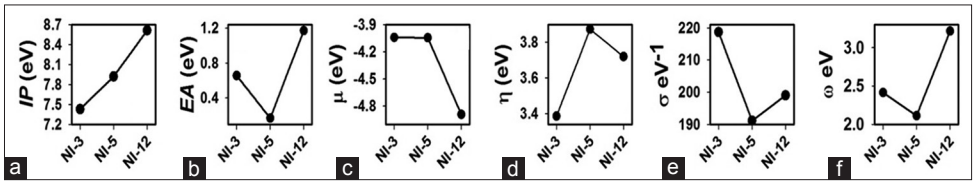

Fig. 3: Plot of ionization potential (a), electron affinity (b), chemical potential (c), chemical hardness (d), chemical softness (e), and electrophilicity index (f) for nilotinib impurity (NI)-3, NI-5, and NI-12. The results are generated in Gaussian and plotted using Sigma Plot v12

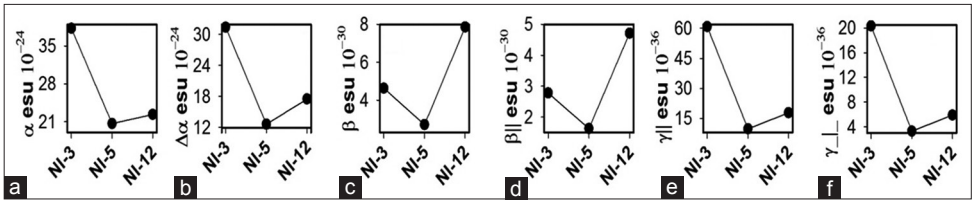

Fig. 4: Plot of polarizability (α) (a), anisotropy of polarizability ($\Delta\alpha$) (b), first (β [c], β //[d]), and second (γ // [e], and γ _|_ [f]) hyperpolarizability for nilotinib impurity (NI)-3, NI-5, and NI-12

Table 6: HOMO, LUMO, and band gap energies for NI-3, NI-5, and NI-12. HOMO and LUMO are directly extracted from the LOG file of the Gaussian optimized structure. The band gap is computed by E_{LUMO}-E_{HOMO}

Molecule	HOMO (eV)	LUMO (eV)	Band gap (eV)
NI-3	−8.83	−5.60	3.23
NI-5	−8.88	−5.07	3.81
NI-12	−8.85	−5.66	3.19

NI: Nilotinib impurity, HOMO: Highest occupied molecular orbitals, LUMO: Lowest unoccupied molecular orbitals

Table 7: Computation of electron affinity, ionization energy, chemical potential, electronegativity, chemical hardness, chemical softness, and electrophilicity index for N and its impurities (NI-3, NI-5, and NI-12). Mean of IP and EA is 7.5 eV and 0.4 eV, respectively [8]

Molecule	All units are in eV						
	IP	***EA***	μ	χ	η	σ	ω
NI-3	7.43	0.66	−4.04	4.04	3.39	218.69	2.41
NI-5	7.92	0.17	−4.04	4.04	3.87	191.14	2.11
NI-12	8.61	1.17	−4.89	4.89	3.72	199.02	3.22

Value deviates from the mean value are highlighted by underline. *IP*: Ionization potential, *EA*: Electron affinity, μ : Chemical potential, χ : Electronegativity, η : Chemical hardness, σ : Chemical softness (=1/η), ω : Electrophilicity index, NI: Nilotinib impurity

the table that *IP* follows the order as NI-12≫NI-5>NI-3. Here, NI-12 is seen to be anomalously high and NI-3 almost similar as the mean value of normal drugs [8]. High *IP* implies low tendency for the formation of the cation. On the other hand, higher the *EA*, greater is the tendency for the formation of an anion. Although, the mean value of EA for normal drugs is ∼0.4 eV, these impurities of N possess high (for NI-12) and low (for NI-5) values of *E*A.

μ, χ, η, σ, and electrophilicity index (ω) properties are also presented in Table 7. All these properties are dependable on *IP* and *EA* (Equation 1 through 4). Few of these properties are also plotted in Fig. 3 (plot C for μ; D for η; E for σ; and F for ω). The η follows the order as NI-5>NI-12>NI-3 (Fig. 5d). σ is the opposite of the η and thus follows the reverse order (Fig. 5e). ω value is plotted in Fig. 3f and noted in Table 7 for NI-3, NI-5, and NI-12. It is seen that ω value follows the similar order as *EA*, i.e., NI-12>NI-3>NI-5.

NLO properties of NIs

Intermolecular interactions such as drug-protein/DNA/RNA are largely understood by DM, α, and first- and second-order hyperpolarizability energy terms [19], which are reliably computed by RB3LYP/6-311G (d,p) level of the theory [10]. How are these parameters affected for N's impurities? To check this above basis set is used and DM, α, and first- and second-rank hyperpolarizability are determined. Isotropic *DM* is presented in Table 8. It is seen that the X and Y components are zero in all the cases with the Z component constituting the total *DM*. Higher and lower DM_{TOTAL} than the reported mean value are highlighted by underline (Table 8). Here, NI-3 and NI-12 show higher and lower DM_{TOTAL}, respectively.

Table 8: Cartesian components and net electric dipole moments (*DM* in Debye) for N's impurities, i.e., NI-3, NI-5, and NI-12

Name	DM_x	DM_y	DM_z	DM_{TOTAL}
NI-3	0.00	0.00	7.79	7.8
NI-5	0.00	0.00	4.77	4.8
NI-12	0.00	0.00	1.46	1.5

Higher and lower values are underlined with respect to the mean of *DM*, which is 4.6 Debye [8]. N: Nilotinib, NI: Nilotinib impurity

Table 9: Components and mean isotropic (α) and anisotropic ($\Delta\alpha$) polarizability (in 10^{-24} esu unit) for N's impurities, i.e., NI-3, NI-5, and NI-12

Name	α_{xx}	α_{yx}	α_{yy}	α_{zx}	α_{zy}	α_{zz}	α	$\Delta\alpha$
NI-3	23.59	9.15	40.98	3.52	7.14	50.15	38.24	31.42
NI-5	22.17	2.21	18.46	−5.71	3.46	21.28	20.64	12.62
NI-12	18.73	−4.05	21.05	−7.50	−3.17	27.25	22.34	17.50

Higher and lower values are underlined with respect to the mean of α, which is 34.0×10^{-24} esu [8]. N: Nilotinib, NI: Nilotinib impurity

α, its components, and anisotropic terms are shown in Table 9. The α of NI-5 and NI-12 is seen to be much lower and that for the NI-3 is slightly higher than the reported mean. In these aspects, NI-3 is seen to be less affected (Table 9). Similar is the case for the anisotropy of polarizability ($\Delta\alpha$) and diagonal components of polarizability (e.g., αXX, αYY, and αZZ), where NI-5 and NI-12 have much lower value than NI-3. Is there any relation of α with chemical reactivity? If molecular hardness (Fig. 3, D) and softness (Fig. 3, E) are compared with the α profile (Fig. 4, A), we see that it is inversely and directly relation with the α (Table 9), respectively. Which of the three impurities is most polarizable and which one is most active chemically?

It is seen that NI-3 is most polarizable (Fig. 4a). It is also seen that it possesses lowest hardness (Fig. 3d) and highest softness (Fig. 3e). Interestingly, the anisotropy of α of NI-3 is also higher than NI-5 and NI-12.

Although, computationally costly, hyperpolarizabilities have been useful molecular descriptor (MD) for drug molecules [20]. We have computed the first- and second-order hyperpolarizability energy terms and presented in Tables 10 and 11, respectively. The first mean hyperpolarizability (β) and its isotropic component (β//) are plotted in Fig. 4c and d, respectively.

The parallel (γ//) and perpendicular (γ_|_) term of the second-order hyperpolarizability are plotted in Fig. 4e and f, respectively. Following points are noteworthy. First, the second-order hyperpolarizability follows a similar pattern as α. Second, the first-order hyperpolarizability is different. Third, the perpendicular component is seen to follow lower range than parallel components for these two-second hyperpolarizability quantities.

Table 10: Components and mean first dipole hyperpolarizability (<β>) and isotropic component of (<β //>) hyperpolarizability (in 10^{-30} esu Unit) for N's impurities, i.e., NI-3, NI-5, and NI-12

Name	β_{xxx}	β_{xxy}	β_{yxy}	β_{yyy}	β_{xxz}	β_{yxz}	β_{yyz}	β_{zxz}	β_{zyz}	β_{zzz}	<β>	β //
NI-3	0.30	1.00	2.22	1.59	0.99	1.42	2.24	−0.02	0.59	−5.48	4.63	2.78
NI-5	−0.96	−0.21	0.26	−0.30	1.48	0.36	−0.65	−1.14	−1.25	0.09	2.71	1.63
NI-12	0.79	0.07	−0.17	0.33	−2.10	0.04	0.00	3.36	0.12	−4.65	7.85	4.71

N: Nilotinib, NI: Nilotinib impurity

Table 11: Components second-ranked parallel (<γ // >) and perpendicular (<γ _|_>) hyperpolarizability (in 10^{-36} esu unit) for N's impurities, i.e., NI-3, NI-5, and NI-12

Name	γ||	γ_|_	γ_{xxxx}	γ_{xxyx}	γ_{xxyy}	γ_{yxyy}	γ_{yyyy}	γ_{xxzx}	γ_{xxzy}	γ_{yxzy}	γ_{yyzy}	γ_{xxzz}	γ_{yxzz}	γ_{yyzz}	γ_{zxzz}	γ_{zyzz}	γ_{zzzz}
NI-3	60.8	20.3	6.6	7.3	11.7	18.5	37.6	3.9	6.1	9.2	16.4	10.7	12.3	19.9	34.4	43.5	175.4
NI-5	9.8	3.3	25.5	−7.0	4.3	−1.7	7.6	−1.5	0.4	−0.3	0.0	1.1	−0.2	1.6	−0.2	−0.8	2.0
NI-12	17.8	5.9	9.1	−1.5	1.0	−1.1	5.2	−10.2	1.2	0.1	−1.8	14.7	−2.3	3.2	−20.8	0.0	36.9

DISCUSSION

In the present study, detailed characterizations of impurities of N such as NI-3, NI-5, and NI-12 are carried out using highly accurate QM procedure. While NI-3 has been reported to be a genotoxic impurity, side effects for the other two are yet to be understood. These impurities occur in trace amount along with the active drug as revealed in the HPLC profile [8,9]. Lipinski's rule of five [17,18] is the first-hand classical MD for the primary characterization of drug and drug-like substances. Largely if a drug shows lower than the upper limit of five molecular properties (Table 2), the molecule is said to be biologically or pharmacologically active in the human body. In other words, the molecule is said to possess druglikeness. N's impurities do not cross the upper limit of the above-mentioned rules. Only one property of an impurity goes below the lower limit. Such a single violation is tolerated [21].

Impurities have differential dihedral and other geometric properties

Experimental or theoretical investigation of molecular properties for these impurities is not yet available. Mutagenic properties and biological activity are related to the chemical reactivity, which, in turn, is dependent on the electronic structure of molecules [22,23,13]. The present study is thus aimed at understanding the electronic structural properties that may have a relation with the genotoxicity of these molecules. Optimization of the impurities is performed without symmetry constraint by RB3LYP/6-311G (d,p) level of theory in Gaussian 09 software package [10]. At this point, mention may be made of the fact that such computation is highly accurate, whose results are closely related to the experimental ones [24]. As far as bond distances and angles are concerned, NI-3, NI-5, and NI-12 show almost identical values among themselves but differ from N. Notably, N is extracted from a complex protein data bank file (3CS9.pdb), where it establishes different kinds of interactions, which could be the reason of such variations. Dihedral or torsion angle is the angle between two planes, which is confined by four atoms and three bond vectors, i.e., in the present case, it is between C1-N1-C3 (plane-A) and N1-C3-C4 (plane-B). It defines the topology of a molecule [25]. It also helps to establish specific interactions in a complex state. The dihedral angle of a ligand may induce a structural change of target molecule in the complex state [26] as the initial (e.g., C1) and the final (e.g., C4) atoms act as the determinant for the dihedral angle. Of three impurities, NI-3, which is known to be genotoxic [27], possesses three rings (thus, two sets of dihedral angles, Table 5), of which one set of dihedral angles is comparable with other impurities (NI-5 and NI-12) and with N (Table 5). The comparable set of dihedral angles for all impurities is higher than that of the parent drug (N), which may indicate differential interactions of impurities with target molecules. Further, interestingly, the same set of dihedral angles for NI-3 is oppositely sensed than other impurities and N, may indicate a different kind of interactions for it. Again, the sets of dihedral angles of NI-3 are largely in oppositely sense also that may point toward the overall compensation of net dihedral angle. In other words, this may increase the planarity of NI-3's ring system. Thus, it seems that NI-3 compared to other impurities possesses topological benefit (see below).

Impurities have differential QM descriptors

DFT is the state of the arts computational method that extracts electronic properties from a given input of chemical systems. It is more so for drugs and drug-like substance [22]. These results approach almost similar values as experimental ones [28]. The method gives an accurate estimate of HOMO and LUMO, which are the indicator of chemical stability and chemical reactivity of a molecule. As these are outermost, they are also called frontier molecular orbital [29]. The donating and accepting ability of electron of a compound could be understood by E_{HOMO} and E_{LUMO}, respectively. On the other hand, chemical reactivity and kinetic stability of a molecule are assessed by the band gap energy [23,28,30]. Notably, NI-12, which has a lowest band gap, is devoid of hydrogen bond donor groups (Table 1). In this respect, NI-5 shows more kinetic stability (Fig. 2c). Notably, E_{HOMO} and E_{LUMO} and band gap are at a lower level for these impurities in comparison to other drug like molecules [31]. Overall, these molecular properties of impurities seem to be relevant for differentiating these from normal drugs.

Electronic and NLO properties of NIs deviate from the mean value of approved drugs

In general, before the experiment, electronic properties are computed to understand the chemical behavior of a molecule [32,22]. *IP* is the amount of energy required to take away one electron from an *M* and *EA*, oppositely, is the amount of energy released when an electron is added to an *M* [23]. μ, χ, η, σ, and electrophilicity index (ω) properties are also used as MDs in the study of drugs [33]. Although all these properties are directly or indirectly dependent on *EA* and *IP*, they reveal additional chemical attributes and information [34]. η is the determinant of chemical stability of a molecule. It is thus equivalent to band gap. Electrophilicity index (ω) is the parameter where two parameters such as μ and η are combined (Equation 5). While the μ is the reactivity of a molecule, hardness is the resistance to the change in electron density of a system or molecule [23]. Thus, it is the stabilization energy of a molecule when it is saturated by an electron from the external environment. A good electrophile is characterized by low η (resistivity to change in electron density) for high *c* (reactivity of a system).

The electric DM is a measure of the separation of positive and negative charges within an *M*. In other words, it is the measure of the net polarity [35]. The dipole α is another important parameter to assess intermolecular interactions. DM and static α could also be useful for the understanding of chemical reactivity and solubility properties [36]. Ligand-protein/DNA interactions are largely characterized by α and hyperpolarizability [37].

In an effort to gain insight into the MDs of clinically approved drugs, based on QM properties, Matuszek and Reynisson (2016) have considered adiabatic *IP*, adiabatic *EA*, *DM*, and α properties. They determined the mean values of these properties using a large database of clinically approved drugs (>1600). The mean value of *IP* and *EA* is 7.5 eV and 0.4 eV, respectively, for most drugs and that for the *DM* and α are 4.6 Debye and 34.0×10^{-24} esu, respectively. Redox stability of drugs is directly related to *IP* and *EA*. On the other hand, the intermolecular interaction between the drug molecule and target protein/DNA and cellular permeability are directly related to *DM* and α properties [38]. Interestingly, the observation of deviation of the above-mentioned properties from the mean value for the impurities (Table 7 and Fig. 3) may indicate that their chemical properties, redox stability, permeability, and interactions with target are greatly affected. Overall, such deviation may lead to the anomalous interaction with cellular components and thereby may raise the possibility of genotoxicity for these impurities.

Planarity of the π-conjugated system, which largely depends on the dihedral properties of rotatable bonds, enhances the mobility of π-electrons [39], and thus makes the drug more active chemically. In the case of NI-5, the planarity is severely affected, which could be the reason for its lowest value of α, $<\Delta\alpha>$, and its diagonal components. Further, the donor group is completely absent in NI-12 (Table 1), which also shows the almost similar deviation of α as NI-5 (Table 9 and Fig. 4). How is the planarity of the ring system of these impurities differentially affected? In these aspects, there exist a discernable difference between NI-3 and NI-5 (also NI-12) (see below). Unlike NI-3, in NI-5 and NI-12, the dihedral angles of the rotatable bond have a counterclockwise sense. In NI-3, the intrastructural dihedral angles (i.e., between A and B and B and C) are in opposite sense (Table 5), i.e., the former is clockwise and the latter is counterclockwise. Thus, in NI-3, the net deviation of planarity seems to be compensated. Taken together, it seems that these fragmented structures of impurities are affecting the α and other properties and thereby altering the biomolecular interactions.

Molecular complexity is the criterion that can be related with $\Delta\alpha$ [29,40]. More the complexity of structure more is the anisotropy of polarizability ($\Delta\alpha$), which is shown in Fig. 4b. NI-3 has relatively more complex structure than the other two impurities and thus $\Delta\alpha$ of the earlier has been more than the latter.

Why are the perpendicular components of α and hyperpolarizability lower than the parallel components? α and hyperpolarizability are affected by structural and geometrical criteria such as the presence of (i) π-conjugate system, (ii) planarity, and (iii) donor and acceptor candidates [41]. Although hydroxyl substitutions are highly advantageous in drugs, as it acts both as a strong donor (through π-bond) and acceptor (through σ-bond), which is completely absent in these impurities. It is known that the perpendicular component is not directly related with π conjugate system [42]. Further, NI-12 harbors only acceptor but no donor groups, which might have a role in the lowering of perpendicular components. Again, the planarity of the ring systems has a role in the contribution to the α and second hyperpolarizability. In this aspect, the first hyperpolarizability is seen to remain unaffected. Taken together, both α and γ but not β are affected by planarity and substituents of the ring system and thus NI-3 is more interactive to biomolecules than other impurities.

CONCLUSION

Electronic structural properties for representative impurities of N are worked out by RB3LYP/6-311G (d, p) level of theory of GAUSSIAN 09 software package. The ground state optimized structures are used for computation of electronic and NLO properties. Corresponding bond lengths and angles of these impurities show remarkable similarity among themselves but show variation from the original drug molecule (N). Compare to N, the dihedral angle between A and B rings of NI-5 and NI-12 is 3 and 2 times, respectively. The corresponding dihedral angle (between A and B rings) of NI-3 (that has A, B, and C rings) found to occur in opposite sense, compare to (i) that of NI-5 or NI-12 and (ii) its own B and C rings, thereby compensating the net non-planarity of the ring system of NI-3. This unique structural feature makes NI-3 more polarizable, hyperpolarizable and chemically more reactive compared to NI-5 and NI-12. In other words, it is more interactive to target molecule. These impurities possess only part of the structure of the parent drug molecule, i.e., N, which by itself is stabilized by strong intramolecular hydrogen bonds. Apart from this structural flexibility, additionally, these impurities are seen to deviate from the mean values of *DM*, α, *IP*, and *EA* of clinically approved drugs may indicate that their interactions with cellular components may lead to an abnormal consequence. The observation of (i) high *EA*, (ii) low band gap, (iii) low η, (iv) high χ, and (v) high *IP* of NI-12 and NI-3 may indicate these impurities are strongly electrophilic in nature. The latter property of these impurities may lead to non-specific binding with DNA, which might be the origin of genotoxicity in these impurities.

ACKNOWLEDGMENT

The author is thankful for the computational facility laboratory of the Department of Biotechnology, The University of Burdwan. Sincere thanks are also due for Prof. Anirban Misra Department of Chemistry, The North Bengal University, and Dr. Amal K. Bandyopadhyay, for Gaussian software and valuable comments for the manuscript.

REFERENCES

1. Kantarjian HM, Giles F, Gattermann N, Bhalla K, Alimena G, Palandri F, *et al.* Nilotinib (formerly AMN107), a highly selective BCR-ABL tyrosine kinase inhibitor, is effective in patients with philadelphia chromosome-positive chronic myelogenous leukemia in chronic phase following imatinib resistance and intolerance. Blood 2007;110:3540-6.
2. Larson RA, Hochhaus A, Hughes TP, Clark RE, Etienne G, Kim DW, *et al.* Nilotinib vs imatinib in patients with newly diagnosed philadelphia chromosome-positive chronic myeloid leukemia in chronic phase: ENESTnd 3-year follow-up. Leukemia 2012;26:2197-203.
3. Beg S, Rizwan M, Sheikh AM, Hasnain MS, Anwer K, Kohli K, *et al.* Advancement in carbon nanotubes: Basics, biomedical applications and toxicity. J Pharm Pharmacol 2011;63:141-63.
4. Bwp DA, Chmp AB. European Medicines Agency Evaluation of Medicines for Human Use 2006.
5. McGovern T, Jacobson-Kram D. Regulation of genotoxic and carcinogenic impurities in drug substances and products. TrAC Trends Anal Chem 2006;25:790-5.
6. Guideline IH. Assessment and Control Of Dna Reactive (Mutagenic) Impurities In Pharmaceuticals To Limit Potential Carcinogenic RISK M7. InInternational Conference on Harmonization of Technical Requirements for Registration of Pharmaceuticals for Human use (ICH): Geneva; 2014 Jun 5.
7. Matuszek AM, Reynisson J. Defining known drug space using DFT. Mol Inform 2016;35:46-53.
8. Schipper PR, Gritsenko OV, Van Gisbergen SJ, Baerends EJ. Molecular calculations of excitation energies and (hyper) polarizabilities with a statistical average of orbital model exchange-correlation potentials. J Chem Phys 2000;112:1344-52.
9. Balaji N, Sultana S. Sensitive determination of related substances in pioglitazone hydrochloride by hplc. Int J App Pharm 2017;9:34-41.
10. Frisch MJ, Trucks GW, Schlegel HB, Scuseria GE, Robb MA, Cheeseman JR, *et al*. Gaussian 09 Revision a 02. Wallingford, CT: Gaussian Inc.; 2009. p. 200.
11. Dennington RD, Keith TA, Millam JM. Gauss View 5.0. Wallingford, CT: 2009.
12. Foresman JB, Frisch A. Exploring chemistry with electronic structure methods: A guide to using Gaussian. Pittsburgh, PA: Gaussian; 1996.
13. Ansary I, Das A, Gupta PS, Bandyopadhyay AK. Synthesis, molecular modeling of N-acyl benzoazetinones and their docking simulation on fungal modeled target. Synth Commun 2017;47:1375-86.
14. Kaduk JA, Zhong K, Gindhart AM, Blanton TN. Crystal structure of nilotinib, C 28 H 22 F 3 N 7 O. Powder Diffr 2015;30:270-7.
15. Weisberg E, Manley PW, Breitenstein W, Brüggen J, Cowan-Jacob SW, Ray A, *et al.* Characterization of AMN107, a selective inhibitor of native and mutant bcr-abl. Cancer Cell 2005;7:129-41.
16. Raghunath M, Singh A, Viswanathan CL. Molecular descriptors and bioactivity scores of 6-substituted benzimidazole-2-carbamates as potential anticancer agents. World J Pharm Pharm Sci 2015;4:1438-4

17. Lipinski CA, Lombardo F, Dominy BW, Feeney PJ. Experimental and computational approaches to estimate solubility and permeability in drug discovery and development settings. Advanced drug delivery reviews 2012;64:4-17.
18. Ghose AK, Viswanadhan VN, Wendoloski JJ. A knowledge-based approach in designing combinatorial or medicinal chemistry libraries for drug discovery 1. A qualitative and quantitative characterization of known drug databases. J Comb Chem 1999;1:55-68.
19. Hurst GJ, Dupuis M, Clementi E. A binitio analytic polarizability, first and second hyperpolarizabilities of large conjugated organic molecules: Applications to polyenes C4H6 to C22H24. J Chem Phys 1988;89:385-95.
20. Zhou T, Huang D, Caflisch A. Quantum mechanical methods for drug design. Curr Top Med Chem 2010;10:33-45.
21. Krauth F, Dahse HM, Rüttinger HH, Frohberg P. Synthesis and characterization of novel 1,2,4-triazine derivatives with antiproliferative activity. Bioorg Med Chem 2010;18:1816-21.
22. Bhatt P, Deepthi S, Kumar CR, Jhaa AN. Facile synthesis, spectral studies, dft calculations and biological activities of novel ni (ii), cu (ii), and pd (ii) complexes of thiadiazole analogs. International Journal of Pharmacy and Pharmaceutical Sciences 2017;9(4);185-92.
23. Pearson RG. The electronic chemical potential and chemical hardness. J Mol Struct THEOCHEM 1992;255:261-70.
24. Woon DE, Dunning Jr. TH. Gaussian basis sets for use in correlated molecular calculations. IV. Calculation of static electrical response properties. J Chem Phys 1994;100:2975-88.
25. Hao MH, Haq O, Muegge I. Torsion angle preference and energetics of small-molecule ligands bound to proteins. J Chem Inf Model 2007;47:2242-52.
26. Ma J, Karplus M. Ligand-induced conformational changes in ras p21: A normal mode and energy minimization analysis. J Mol Biol 1997;274:114-31.
27. Kompella A, Rao AK, Rachakonda S, Gampa VK, Nannapaneni VC. Inventors; Natco Pharma Ltd, Assignee. Process for the Preparation of Nilotinib. United States Patent US 9,061,028. 2015 Jun 23.
28. Stiehler J, Hinze J. Calculation of static polarizabilities and hyperpolarizabilities for the atoms He through Kr with a numerical RHF method. J Phys B At Mol Opt Phys 1995;28:4055.
29. Chen L, Lu J, Huang T, Cai YD. A computational method for the identification of candidate drugs for non-small cell lung cancer. PLoS One 2017;12:e0183411.
30. Aihara JI. Reduced HOMO-LUMO gap as an index of kinetic stability for polycyclic aromatic hydrocarbons. J Phys Chem A 1999;103:7487-95.
31. Obot IB, Obi-Egbedi NO, Umoren SA. Antifungal drugs as corrosion inhibitors for aluminium in 0.1 M HCl. Corrosion Science 2009;51(8):1868-75.
32. Ghanadzadeh A, Ghanadzadeh H, Ghasmi G. On the molecular structure and aggregative properties of Sudan dyes in the anisotropic host. J Mol Liq 2000;88:299-308.
33. Zhan CG, Nichols JA, Dixon DA. Ionization potential, electron affinity, electronegativity, hardness, and electron excitation energy: Molecular properties from density functional theory orbital energies. J Phys Chem A 2003;107:4184-95.
34. Xue Y, Li ZR, Yap CW, Sun LZ, Chen X, Chen YZ, *et al.* Effect of molecular descriptor feature selection in support vector machine classification of pharmacokinetic and toxicological properties of chemical agents. J Chem Inf Comput Sci 2004;44:1630-8.
35. Harris PG, Baker CA, Green K, Iaydjiev P, Ivanov S, May DJ, *et al*. New experimental limit on the electric dipole moment of the neutron. Phys Rev Lett 1999;82:904.
36. Lim IS, Pernpointner M, Seth M, Laerdahl JK, Schwerdtfeger P, Neogrady P, *et al*. Relativistic coupled-cluster static dipole polarizabilities of the alkali metals from Li to element 119. Phys Rev A 1999;60:2822.
37. Hansch C, Steinmetz WE, Leo AJ, Mekapati SB, Kurup A, Hoekman D, *et al.* On the role of polarizability in chemical-biological interactions. J Chem Inf Comput Sci 2003;43:120-5.
38. Boger DL, Desharnais J, Capps K. Solution-phase combinatorial libraries: Modulating cellular signaling by targeting protein-protein or protein-DNA interactions. Angew Chem Int Ed Engl 2003;42:4138-76.
39. Lee JY, Kim KS, Mhin BJ. Intramolecular charge transfer of π-conjugated push-pull systems in terms of polarizability and electronegativity. J Chem Phys 2001;115:9484-9.
40. Gresh N, Cisneros GA, Darden TA, Piquemal JP. Anisotropic, polarizable molecular mechanics studies of inter- and intramolecular interactions and ligand-macromolecule complexes. A Bottom-up strategy. J Chem Theory Comput 2007;3:1960-86.
41. Ghanadzadeh A, Zakerhamidi MS, Tajalli H. Electric linear dichroism study of some Sudan dyes using electro-optic and spectroscopic methods. J Mol Liq 2004;109:143-8.
42. Lazzeretti P. Assessment of aromaticity via molecular response properties. Phys Chem Chem Phys 2004;6:217-23.